

Research Article

Open Access

Engineering Iodine-Containing 3D-Crosslinked Methacrylic Microspheres for Transarterial Embolization. Evaluation of Fluoroscopic (X-Ray) Visibility in a Hospital Setting

Abderazak Benzina¹, Roeland Heijboer², Leo H. Koole^{*3}

¹Interface BIOMaterials BV, Markt 68, Melick, The Netherlands

²Zuyderland Medical Center Parkstad, Department of Medical Imaging, Henri Dunantstraat 5, 6419 PC Heerlen, The Netherlands

³School of Engineering, Department of Chemical Engineering, Nazarbayev University, Astana, Kazakhstan

Corresponding Author: Leo H. Koole, School of Engineering, Department of Chemical Engineering, Nazarbayev University, Astana, Kazakhstan. **Email:** koole.leo@gmail.com

Citation: Leo H. Koole et al.(2017), Engineering Iodine-Containing 3D-Crosslinked Methacrylic Microspheres for Transarterial Embolization. Evaluation of Fluoroscopic (X-Ray) Visibility in a Hospital Setting. Int J Nano Med & Eng. 2:11, 171-176.

DOI:10.25141/2474-8811-2017-11.0184

Copyright: ©2017 Leo H. Koole et al. This is an open-access article distributed under the terms of the Creative Commons Attribution License, which permits unrestricted use, distribution, and reproduction in any medium, provided the original author and source are credited

Received: November 21, 2017; **Accepted:** November 30, 2017; **Published:** December 20, 2017

Abstract:

Transarterial chemo-embolization (TACE) provides a successful treatment mode for some benign or malignant tumors. The success of TACE is largely due to (i), development of excellent instruments and techniques for real-time X-ray imaging, and (ii), advanced catheters which allow for accurate intra-arterial navigation. Further improvements can –most probably- be achieved by enhancing the functionality of the embolic particles. For example, embolic particles can be made radiopaque, which means that they can be visualized in situ through X-ray fluoroscopy and computed tomography (CT). X-ray visibility of the radiopaque 3D-crosslinked methacrylic iodine-containing embolic microspheres of the new embolization product X-Spheres was evaluated. A rabbit cadaver model and state-of-the-art imaging equipment in a hospital setting were used. Clear visibility of the particles was found in CT images, especially if the plane of vision is chosen in such that overlap with bone structures is avoided. Therefore, the use of radiopaque embolic microspheres can provide important and otherwise inaccessible post-procedural information about the efficacy of the procedures

Dispersed radiopaque microspheres



Keywords: Radiopacity, Microspheres, Embolization, X-Ray Visibility

Introduction

Transcatheter arterial chemoembolization (TACE), using polymer embolic microspheres, is rapidly gaining importance in clinical practice.¹ For a growing number of pathologies, TACE can provide a minimally invasive therapeutic alternative to surgery. The technique can bring significant advantages, such as faster recovery and reduction of treatment cost. For example, TACE is now widely used to treat patients with uterine fibroids (leiomyomata).²⁻⁴ These are benign tumours, growing in the wall of the uterus. TACE preserves the uterus, and recent studies showed that women without further infertility factors demonstrate an encouraging capacity to deliver after uterine artery embolization.⁵ This is in sharp contrast with the standard therapy for the treatment of uterine fibroids, which is surgical excision of the uterus (also known as hysterectomy). Furthermore, patient recovery from TACE is much faster and easier, in comparison with recovery from hysterectomy.⁶ Many more examples of the growing importance of TACE can be found in oncology. TACE has now become the preferred technique for the treatment of hepatocellular carcinoma (HCC).^{7,8} The newest forms of TACE in oncology use drug-eluting embolic microspheres. These particles do not only embolize part of the tumour's vascular tree, they also locally deliver a cytostatic agent (such as doxorubicin), or a low-molecular-mass multi-tyrosine kinase inhibitor such as sorafenib (also known as NexavarR) or vandetanib, in a controlled manner.⁹⁻¹²

Embolic microspheres are of scientific and technical interest. Per se, the particles have a mere passive function: they are designed to flow with the arterial bloodstream into the arterial vessel tree of the tumour until they get stuck, thus blocking influx of fresh arterial blood. Ideally, this leads to starving the tumor of oxygen and nutrients in the downstream area, causing ischaemic necrosis.¹³ A challenging hypothesis is that adding more functionalities to embolic microspheres may enhance efficacy and/or safety of TACE. Obviously, using the embolic particles as a vehicle for sustained local drug release is an important example of such an additional functionality. Another example is the development of radiopaque embolic microspheres. Such particles absorb X-radiation and are –therefore- visible on X-ray images. This idea is rather straightforward, since TACE is normally executed under real-time X-ray fluoroscopic guidance. A priori, the use of radiopaque embolic microspheres has several interesting potential advantages: (i), the radiopaque embolic particles can be monitored, during the TACE procedure and afterwards; (ii), use of radiopaque embolic particles might lower the risk for particle reflux, i.e. unintended embolization of healthy tissues; (iii), use of radiopaque embolic particles could open possibilities to use less contrast agent in TACE procedures; this would not only save cost, it would also reduce the risk for X-irradiation-related DNA damage (e.g., in circulating blood cells).¹⁴

While dozens of scientific studies on radiopaque embolic particles for TACE were published, it appears that there are currently two developments with significant progress regarding translation into clinical applications. Both are being pursued predominantly in industry. The approaches are conceptually similar, since both

are using iodine as the radiopaque element, and in both cases the particles are inherently radiopaque since the iodine atoms are covalently bound to the bead's 3D-crosslinked polymer matrix. This follows, in essence, the same principle as is found in the clinically used X-ray contrast agents: these are concentrated solutions of organic compounds containing covalently linked iodine (such as the well-known non-ionic contrast agent iopamidol) in water.

One development is essentially an extension/refinement of the well-known DC Bead™ hydrogel formulation.¹⁵ In short, the formulation consists (in part) of poly(vinylalcohol), and iodine is introduced through reaction with 2,3,5-triiodobenzaldehyde leading to stable cyclic acetal linkages with pendant triiodobenzoyl moieties. It was found that iodine is homogeneously distributed throughout the volume of these so-called DC bead LUMITM microspheres; the iodine content is approximately 150 mg iodine/mL sedimented beads. Noteworthy, DC bead LUMITM microspheres can also be loaded with different cytostatic and angiogenic agents, thus not only acting as embolic particles, but also as temporary vehicles for controlled intratumoral release of the drug.^{16,17}

The other development was described by ourselves, and concerns the CE-marked radiopaque embolization product X-Spheres™.^{18,19} These radiopaque microspheres are manufactured in a one-step synthetic procedure, and they consist of a three-dimensional macromolecular network of the poly(methacrylate) type. One of the reactive monomers is 2-(4-iodobenzoyl)-ethyl methacrylate (abbreviated as 4-IEMA), which is a methacrylate structure having covalently bound iodine in its sidegroup. 4-IEMA easily reacts with other methacrylates such as methylmethacrylate (MMA), hydroxyethyl methacrylate (HEMA) and the crosslinker tetraethyleneglycol dimethacrylate (TEGDMA)^{18,19}

In this article, we present an experimental model study that produced representative X-ray images of the radiopaque embolic microspheres, in 7 different diameter ranges, of the product X-Spheres. The images were recorded using the X-ray fluoroscopic imaging equipment in a state-of-the-art hospital cath lab (plain X-ray fluoroscopy). Furthermore, computer tomography (CT) X-ray images of the same model were measured. Although our model (a rabbit cadaver) was significantly smaller than the human body, the data allowed us to conclude that the radiopaque microspheres will also be clearly visible on CT images after intra-arterial deposition in patients. The clear visibility of the embolic microspheres in situ is likely to provide a new access route toward potentially important information (for evaluation of TACE procedures) that can be derived from post-procedural imaging.

Materials and Methods

This study was performed with radiopaque embolic microspheres as produced by the company INterface BIOmaterials BV (Melick, The Netherlands, product X-Spheres™). The particles were available in 7 different sizes (diameter ranges). These are: 125-200 μm, 200-250 μm, 250-300 μm, 300-400 μm, 400-600 μm, 600-710 μm, and 710-850 μm. The particles contain approximately 3 % iodine (by mass).

At the onset of the study we sought for a practical model that

would yield representative and meaningful data regarding the X-ray visibility of the embolic microspheres. We reasoned as follows: the model should be suitable to record the images under clinical conditions, i.e. it should be possible to really take the model with the embolic microspheres implanted in it to a state-of-the-art modern catheterization lab, and to record images there. Moreover, the model should also allow for straightforward comparison of the radiopacity of the microspheres on one hand, and the radiopacity of neighbouring bone structures on the other hand. Furthermore, the model should allow us to evaluate the X-ray visibility of the microspheres in a slightly dispersed situation. Note that, after real embolization, embolic microspheres will also be more or less separated and spread throughout the targeted vessel bed.

The model that was chosen eventually was a rabbit cadaver, which was purchased in a local butcher shop (it was intended for human consumption). Furthermore, we decided to implant the embolic microspheres in portions of 100 mg. Prior to implantation, embolic

microspheres were weighed and mixed with butter (0.5 g) at room temperature. Butter, consisting of merely organic fat and water, provides a suitable soft tissue mimic (radiolucent), and the butter/microsphere mixture assures a certain degree of dispersion (20 %) of the microspheres. To facilitate implantations, the butter/microsphere mixtures were transferred into a cylindrical plastic molds (diameter 10 mm, height 5 mm) using a spatulum, and frozen (-20 °C) to harden.

During the implantations (which did not require sterile conditions), the rabbit model was exposed on a laboratory table (viz. Fig. 1a). The butter/microsphere mixtures were released from their plastic moulds, yielding hard button-like structures, which could be implanted easily (viz. Fig. 1b). The incisions were then closed with a few stitches (viz. Fig. 1c). The model comprised 14 sites of sufficient amount of soft tissue for the implantation of a butter/microsphere button.



Figure 1: (a) Illustration of the experimental model for the evaluation of the X-ray visibility of the embolic microspheres, which is a rabbit cadaver. (b) Implantation of one of the microsphere specimens (see text).

In total, 14 buttons (two of each diameter range, vide supra) were implanted, e.g. in the hind limbs, on the back, and in the shoulder regions. Subsequently, the model was packed in a closed plastic bag, and kept frozen (-20 °C) until images could be recorded. X-ray imaging was performed in the Zuyderland Hospital (Heerlen, the Netherlands), in two sessions, both under the responsibility of RH (see author list). The first session was carried out in the hospital's cath lab, with a Philips EasyDiagnost Eleva DRF digital radiography/fluoroscopy instrument. This yielded a set of plain X-ray fluoroscopy images, from which the X-ray visibility of the respective microspheres could be evaluated. The second session was carried out in the hospital's facility for computed X-ray tomography (CT), with Philips IQon Spectral CT system. A large

series of cross-sectional X-ray fluoroscopic images was acquired here. X-ray visibility of the respective particles could be evaluated in more detail from these images.

Results

Figure 2 shows two representative X-ray images from the first imaging session (angiography suite, plain fluoroscopic images). Image (a) clearly shows clustered embolic microspheres in two regions (arrows). The arrow in the upper left part of image (a) points at a collection of radiopaque microspheres in the diameter range 300-400 µm; these are in the middle size of the microspheres in our study. Note that these particles are too small to be discerned individually. The arrow in the lower right part of image (a) points at a

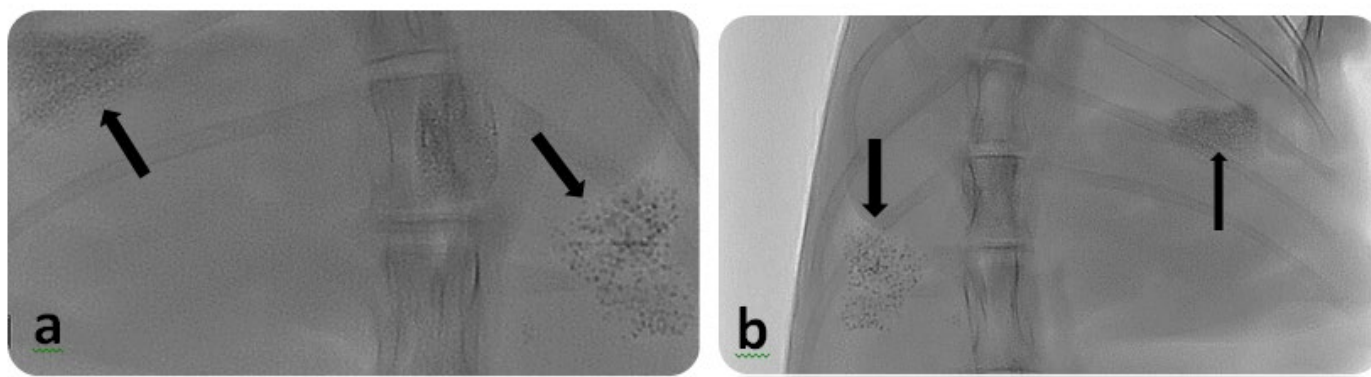


Figure 2: Plain fluoroscopic X-ray images, recorded under realistic hospital conditions, showing clusters of the radiopaque microspheres of the product X-Spheres in situ.

cluster of slightly larger radiopaque microspheres; these are in the diameter range 600 – 700 μm . These particles can be seen individually. Analogously, in image (b), the left arrow points down at a cluster of microspheres in the diameter range 400-600 μm , and the right arrow points upward to a cluster of microspheres in the diameter range 200-250 μm .

Clearly, in some cases, the X-ray beam was attenuated by two or more adjacent microspheres, which locally enhanced the contrast; this is, for instance, the case in the right cluster of microspheres in Figure 2 (a). In addition, Figure 2 reveals that the contrast generated by the microspheres is comparable to the contrast of the rabbit's bone structures (spine, ribs). It must be noted that images of the radiopaque microspheres in Figure 2 are, actually, artificial and

representing an ideal situation: there is no image overlap with any bone structure of the animal's anatomy. This will not be encountered in clinical practice, since the anatomy is much more complex then, and overlap with bone-derived structures in X-ray images is inevitable. For instance, this would be the case for uterine artery embolizations, since these X-ray images would certainly be dominated by local bone structures such as the spine and pelvic bone. The images in Figure 3 are derived from the series CT measurements which we recorded subsequently.

Note that these images actually show cross sections of the animal; image 3a is a cross section close to the animal's neck, while image 3b is a cross-section that was taken just below the hip joints.

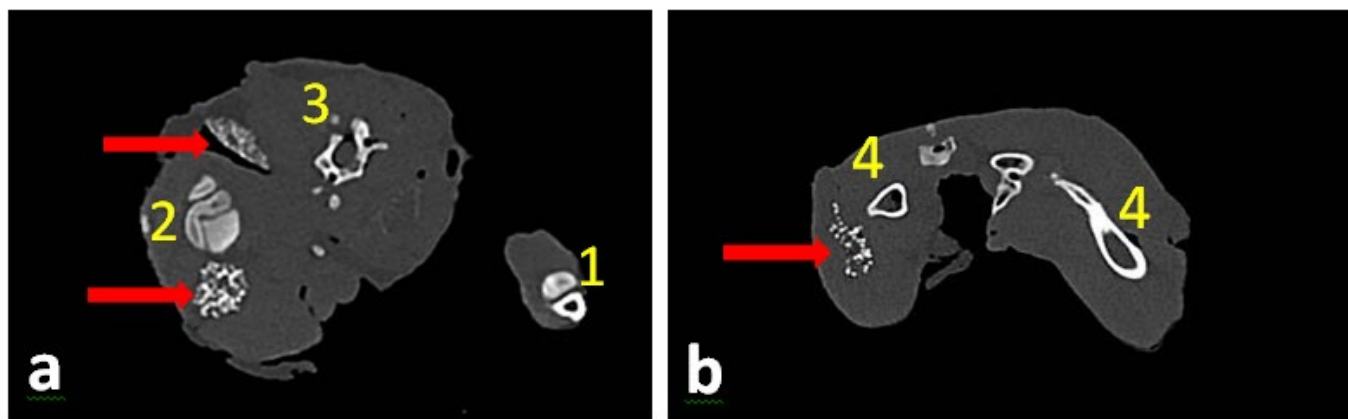


Figure 3: Cross-sectional CT images of the rabbit model. Image (a) refers to the animal's neck region. Image (b) to the animal's bottom. Both cross-sections show clusters of radiopaque microspheres of different diameter size, as well as anatomical features (see text).

In Figure 3a, the most prominent anatomical features are the left radius and ulna (1), the right shoulder (2) and the spine (3). In addition, cross-sectional images of two clusters with microspheres are seen (red arrows). The lower cluster consists of radiopaque microspheres in the diameter range 710 – 850 μm ; these are the largest microspheres from our study. The higher cluster consists of radiopaque microspheres in the diameter range 300-400 μm (intermediate size). Note that both regions of microspheres are clearly visible, although the particles cannot be discerned individually. In addition, note that the black area adjacent to the 300-400 μm diameter microspheres reflects that some air was included in the implantation cavity during implantation.

In Figure 3b, the most important anatomical features are the left and right femura (4). The red arrow in (b) also points at radiopaque microspheres which are implanted in the left thigh. The particles are clearly dispersed, and can be seen individually; these diameters of these microspheres are in the range 710-850 μm .

Discussion

This study sheds new light on the important question whether the X-ray contrast of our crosslinked methacrylic microspheres, containing covalently bound iodine, will generate sufficient X-ray contrast to enable their monitoring or localization during or after TACE treatment of patients. Obviously, the X-ray visibility during plain angiography is weak, especially for the relatively small-sized microspheres. There are two factors to consider, namely (i), that there will inevitably be overlap of bone structures and embolic microspheres in the fluoroscopic images which are seen during TACE of a patient, and (ii), that the embolic microspheres are dispersed in contrast fluid during the injection phase of TACE. Hence, it seems clear that the real-time fluoroscopic images will not show the embolic microspheres of the product X-Spheres flowing through the catheter's lumen or through the target arterial branches. Hence, it must be concluded that the use of radiopaque embolic microspheres per se, will not be helpful in the determination of the TACE endpoint, nor in the prevention of reflux.

However, the observation that the radiopaque microspheres are clearly visible in CT images (Fig. 4) is, in our opinion, important. Images of (clusters of) microspheres in CT slice-images are not disturbed by over- or underlying bone structures, provided that the orientation of the slice is chosen carefully. Hence, the CT data on our rabbit model imply that the particles would also be visible if the surrounding anatomy became complex. We envisage that this feature can be important for several post-procedural assessments. Localization of the embolic microspheres can provide insight as to whether the TACE procedure has indeed led to tissue necrosis inside the tumor.

Conclusion

The X-ray imaging data generated with the rabbit cadaver model and state-of-the-art hospital imaging equipment, indicate that the visibility of the radiopaque microspheres is insufficient for per-procedural real-time tracking of the embolic particles during TACE. Yet, the X-ray visibility of the embolic particles in CT images is excellent, and there is no doubt that the same degree of visibility will be achieved for these embolic particles inside a human patient. These findings imply that the radiopaque microspheres of

the product X-Spheres can be localized and observed by clinical CT, and this provides a basis for a new type of post-procedural follow-up of embolization procedures.

References

1. "Embolization" Springer 2014; Chabrot P and Boyer L, Eds. ISBN 9781447151814
2. Kröncke, T.; David, M. *Uterine Artery Embolization (UAE) for Fibroid Treatment: Results of the 6th Radiological Gynecological Expert Meeting*. *Geburtshilfe Frauenheilkd.* 2017, 77(6): 689-692.
3. de Bruijn, A.M.; Smink, M.; Lohle, P.N.M.; Huirne, J.A.F.; Twisk, J.W.R.; Wong, C.; Schoonmade, L.; Hehenkamp, W.J.K. *Uterine Artery Embolization for the Treatment of Adenomyosis: A Systematic Review and Meta-Analysis*. *J Vasc Interv Radiol.* 2017, Oct 9.
4. de Bruijn, A.M.; Smink, M.; Hehenkamp, W.J.K.; Nijenhuis, R.J.; Smeets, A.J.; Boekkooi, F.; Reuwer, P.J.H.M.; Van Rooij, W.J.; Lohle, P.N.M. *Uterine Artery Embolization for Symptomatic Adenomyosis: 7-Year Clinical Follow-up Using UFS-Qol Questionnaire*. *Cardiovasc Intervent Radiol.* 2017, 40, 1344-1350.
5. Torre, A.; Fauconnier, A.; Kahn, V.; Limot, O.; Bussières, L.; Pelage, J.P. *Fertility after uterine artery embolization for symptomatic multiple fibroids with no other infertility factors*. *Eur Radiol.* 2017, 27, 2850-2859.
6. de Bruijn, A.M.; Ankum, W.M.; Reekers, J.A.; Birnie, E.; van der Kooij, S.M.; Volkers, N.A.; Hehenkamp, W.J. *Uterine artery embolization vs hysterectomy in the treatment of symptomatic uterine fibroids: 10-year outcomes from the randomized EMMY trial*. *Am J Obstet Gynecol.* 2016 215, 745.
7. Magistri, P.; Tarantino, G.; Ballarin, R.; Berretta, M.; Pecchi, A.; Ramacciato, G.; DI Benedetto, F. *The Evolving Role of Local Treatments for HCC in the Third Millennium*. *Anticancer Res.* 2017, 37:389-401.
8. Lanza, E.; Donadon, M.; Poretti, D.; Pedicini, V.; Tramarin, M.; Roncalli, M.; Rhee, H.; Park, Y.N.; Torzilli, G. *Transarterial Therapies for Hepatocellular Carcinoma*. *Liver Cancer.* 2016, 6, 27-33
9. Pesapane, F.; Nezami, N.; Patella, F.; Geschwind, J.F. *New concepts in embolotherapy of HCC*. *Med Oncol.* 2016, 217, 34(4):58.
10. Wang, Y.; Benzina, A.; Molin, D.G.M.; van den Akker, N.M.S.; Gagliardi, M.; Koole, L.H. *Preparation and structure of drug-carrying biodegradable microspheres designed for transarterial chemoembolization therapy*. *J. Biomater. Sci.* 2015, 26, 77-91.
11. Wang, Y.; Molin, D.G.M.; Sevin, Ch.; Grandfils, C.; van den Akker, N.M.S.; Gagliardi, M.; Knetsch, M.L.W.; Delhaas, T.; Koole, L.H. *In vitro and in vivo evaluation of drug-eluting microspheres designed for transarterial embolization therapy*. *Int. J. Pharm.* 2016, 503, 150-162.
12. Hagan, A.; Phillips, G.J.; Macfarlane, W.M.; Lloyd, A.W.; Czuczman, P.; Lewis, A.L. *Preparation and characterisation of vandetanib-eluting radiopaque beads for locoregional treatment of hepatic malignancies*. *Eur J Pharm Sci.* 2017, 101:22-30.
13. Bruix, J.; Sala, M.; Llovet, J.M. *Chemoembolization for hepatocellular carcinoma*. *Gastroenterology* 2004, 127, S179-188.

14. Harbron, R.; Ainsbury, E.A.; Bouffler, S.D.; Tanner, R.J.; Eakins, J.S.; Pearce, M.S. *Br. J. Radiol.* 2017, 90, 1079.
15. Lewis, A.L. **DC Bead TM: a major development in the toolbox for the interventional oncologist.** *Expert Rev. Med. Devices* 2009, 6, 389-400.
16. Ashrafi, K.; Tang, Y.; Britton, H.; Domenge, O.; Blino, D.; Bushby, A.J.; Shuturminska, K.; den Hartog, M.; Radaelli, A.; Negussie, A.H.; Mikhail, A.S.; Woods, D.L.; Krishnasamy, V.; Levy, E.B.; Wood, B.J.; Willis, S.L.; Dreher, M.R.; Lewis, A.L. **Characterization of a novel intrinsically radiopaque Drug-eluting Bead for image-guided therapy: DC Bead LUMI™.** *J Control Release* 2017, 250:36-47.
17. Hagan, A.; Phillips, G.J.; Macfarlane, W.M.; Lloyd, A.W.; Czuczman, P.; Lewis, A.L. **Preparation and characterisations of vandetanib-eluting radiopaque beads for locoregional treatment of hepatic malignancies.** *Eur. J. Pharm. Sci.* 2017, 101, 22-30.
18. Benzina, A.; Aldenhoff, Y.B.; Heijboer, R.; Koole, L.H. **Translational Development of Biocompatible X-Ray Visible Microspheres for Use in Transcatheter Embolization Procedures.** *J Material Sci Eng* 5 2016, 238. doi:10.4172/21690022.1000238
19. Saralidze, K.; Knetsch, M.L.; van Berkel, R.G.; Mostert, C.; Koole, L.H. **Radiopaque microspheres for improved transarterial chemical embolization (TACE).** *J Control Release.* 2011;152 Suppl 1:e74-5. doi: 10.1007/s12032-017-0917-2. Epub 2017 Mar 16. Review.